AD NUMBER
AD845056
LIMITATION CHANGES

TO:

Approved for public release; distribution is unlimited.

FROM:

Distribution authorized to U.S. Gov't. agencies and their contractors; Critical Technology; 10 OCT 1968. Other requests shall be referred to Naval Ordnance Laboratory, White Oak, Silver Spring, MD. This document contains export-controlled technical data.

AUTHORITY

NOL ltr, 15 Nov 1971

SUPERSONIC WIND TUNNEL MAGNUS
MEASUREMENTS OF THE 7-, 8-, 9- AND
10-CALIBER ARMY-NAVY SPINNER
PROJECTILE

DEC 23 1968

A

NOL

10 OCTOBER 1968

UNITED STATES NAVAL ORDNANCE LABORATORY, WHITE OAK, MARYLAND

AD 845056

SUPERSONIC WIND TUNNEL MAGNUS MEASUREMENTS OF THE 7-, 8-, 9- AND 10-CALIBER ARMY-NAVY SPINNER PROJECTILE

Prepared by:

John E. Holmes
Frank J. Regan
Mary Ellen Falusi

ABSTRACT: The Army-Navy Spinner Projectile is a research shape that has been used as the foundation of many spin stabilized weapon designs. The purpose of the wind tunnel tests was to make supersonic wind tunnel Magnus measurements on AN Spinner configurations of 7-, 8-, 9- and 10-caliber lengths. Such an experimental study indicates the effect of length on the Magnus force and moment for a basic spin stabilized shape.

U. S. NAVAL ORDNANCE LABORATORY
White Oak, Silver Spring, Maryland

i

NOLTR 68-172   10 October 1968

SUPERSONIC WIND TUNNEL MAGNUS MEASUREMENTS OF THE 7-, 8-, 9- AND
10-CALIBER ARMY-NAVY SPINNER PROJECTILE

The purpose of this investigation was to obtain the supersonic
Magnus force and moment characteristics of the Army-Navy Spinner
Projectile in 7-, 8-, 9- and 10-caliber lengths.

This project was performed at the request of the Naval Weapons
Laboratory under task number A32 320/292/69F 20311202 WU-3.

                              E. F. SCHREITER
                              Captain, USN
                              Commander

                              L. H. Schindel
                              L. H. SCHINDEL
                              By direction

CONTENTS

ILLUSTRATIONS

INTRODUCTION

The Army-Navy Spinner Projectile is a basic research shape composed of an ogival nose and a cylindrical afterbody. From the measured aerodynamic characteristics of this shape, performance estimates can be made of practical spin stabilized weapon designs. The wind tunnel measurements in this report present the supersonic Magnus characteristics of the AN spinner configuration having several body lengths. Since long (over 5 calibers) shapes have current operational interest, spinners of 7-, 8-, 9- and 10-caliber lengths have been chosen for investigation. Measurements were made at three supersonic Mach numbers: 2.0, 2.3 and 2.7. Since these measurements were made on four body lengths, the significant result of this study is a presentation of the effect of afterbody length on the supersonic Magnus characteristics of a slender spin stabilized configuration.

One of the main purposes for studying length effects is that long projectiles are of current interest as a spin stabilized rocket assisted weapon. The extra length is required for storage of booster and sustainer propellants. It is conceivable that such a spin stabilized round might be launched from a tubular launcher on a airborne platform. Figure 1 illustrates one such type of weapon employment.

Figure 1 also indicates the type of measurements made during this investigation. The normal force, C_N, pitching moment, C_m,

side force, C_y, and yawing moment, C_n, coefficients were measured

for various angles of attack, spin rates and Mach numbers. It was established that the side force and yawing moment were linear functions of spin rate; therefore, these data are presented as slopes of side force and yawing moment with spin rate. It is these slopes which are defined as the Magnus force and moment derivatives.

All wind tunnel tests were carried out in the Naval Ordnance Laboratory's Supersonic Tunnel No. 1. The range of test variables was as follows: The spin rate varied from 50 to 500 revolutions per second, the angle of attack from 0 to an upper limit which varied around a nominal value of 16 degrees and Mach numbers of 2.0, 2.3 and 2.7.

SYMBOLS

cp	center of pressure
C_m	static pitching moment coefficient, My/QSd
C_n	yawing moment coefficient, Mz/QSd

1

c_{n_p}	Magnus moment derivative, derivative of the yawing moment with respect to reduced frequency, $\partial C_n / \partial (pd/2V)$
C_N	normal force coefficient, F_z/QS
c_y	side force coefficient, F_y/QS
c_{y_p}	Magnus force derivative, derivative of the side force with respect to reduced frequency, $\partial C_y / \partial (pd/2V)$
d	reference length, body diameter
F_x	component of aerodynamic force along x axis
F_y	component of aerodynamic force along y axis
F_z	component of aerodynamic force along z axis
M	Mach number
M_x	rolling moment, moment about x axis
M_y	pitching moment, moment about y axis
M_z	yawing moment, moment about z axis
p	spin rate
$\tilde{p}$	reduced frequency, $pd/2V_\infty$
P_o	free-stream stagnation pressure
Q	dynamic pressure, $1/2 \ \rho V_\infty^2$
r	distance of center of pressure from center of gravity
r_m	moment arm of Magnus force
r_s	moment arm of static force
R	gas constant for air
R_e	Reynolds number (based upon body length)
$R_{e/\ell}$	Reynolds number per foot of body length
S	reference area, $\pi d^2/4$

T	static temperature
T_O	total temperature
V	velocity vector of body's center of gravity
V_∞	free-stream velocity
x	body axis from center of gravity to nose along longitudinal axis of symmetry
y	body axis orthogonal to x and normal to the angle of attack plane.
z	body axis orthogonal to the x and y axis
α	angle of attack
ρ	density of the free stream

DESCRIPTION OF CONFIGURATIONS

Figure 2 shows the four slender bodies used in the wind tunnel Magnus measurements. These models were formed by adding cylindrical afterbodies to the secant ogive nose. Afterbody lengths were 5-, 6-, 7- and 8-calibers, which when added to the 2-caliber nose, formed the 7-, 8-, 9- and 10-caliber slender body configurations.

The basic configuration used for these slender bodies is the AN Spinner Projectile. Figure 3 shows the wind tunnel model with appropriate dimensions for the 7-caliber version. It will be noted that a nominal 8.5-caliber radius, 2-caliber long secant ogival nose is added to a 5-caliber afterbody to make a configuration of 7-calibers in overall length. Figure 4 illustrates the assembled 7-caliber slender body mounted on the wind tunnel Magnus balance.

EXPERIMENTAL METHOD

Magnus measurements in a wind tunnel are quite similar to the more conventional static measurements. The main difference is that in a Magnus test the model must spin. Therefore, provision must be made both for driving the model and for providing a bearing system which greatly restricts even slight model angularity with respect to the balance. Thus, while the model must have complete freedom to spin, it must be attached as rigidly to the balance as a model in a conventional static aerodynamic test.

3

Another difficulty arises which is inherent in the Magnus effect itself. The Magnus force acts at right angles to the angle of attack plane and is roughly an order of magnitude less than the corresponding normal force. Alternately stated, the Magnus force must be measured in the presence of an orthogonal normal force which is approximately ten times greater. The inescapable conclusion then, is that the Magnus balance must be far more sensitive in yaw than it is in pitch. One important consideration here is that this sensitivity must not be obtained at the expense of a great reduction in balance yaw rigidity. Quite obviously a large reduction in the balance's yaw moment of inertia could provide sufficient yaw sensitivity. The difficulty encountered here is that the ensuing loss of balance rigidity could easily result in excessive model yaw vibrations during a test. The goal of the balance design, then, is to effect a compromise between decreasing balance rigidity and increasing balance sensitivity.

The heart of the Magnus balance is its sections to which the yaw gages are attached. Figure 5 is an illustration of the forward gage section as seen in the pitch plane. Figure 6 is essentially the same section except that the view is of the yaw plane. From both of these photographs it can be seen that the yaw gages are located on a bridge-like section attached to the balance proper by means of a thin necked-down section. In examining figures 5 and 6 it can be seen that the balance has a somewhat reduced cross section in the yaw direction as compared to that in the pitch direction. However, this area reduction is only responsible in part for the balance's yaw sensitivity. Of equal importance are the Magnus bridges themselves.

Figure 7 indicates how this Magnus bridge functions. The balance is assumed to be under a yaw moment of such a sign that the upper fibers of the beam are under compression while the lower fibers are under tension. Since the elastic axis of the Magnus bridge is not collinear with its point of attachment to the balance proper, the effect of the compression (or tension) is to induce secondary bending in the bridges. Thus, in response to the bending in the balance proper, the Magnus bridges in undergoing secondary bending act as mechanical amplifiers. In order to maximize the curvature of the Magnus bridge, or equivalently its bending moment, the points of attachment to the balance proper should approximate pin-joints as closely as possible. Hence, the necked-down sections at the point of attachment between bridge and balance proper are utilized to obtain the advantages of a pin-joint by permitting the maximum bending of the Magnus bridge.

As mentioned previously, the Magnus support system must provide the means for attaching and spinning the model as well as the usual provisions of a static balance. Figure 8 indicates some of the internal features of the Magnus wind tunnel support system. It will be noted in this figure that the model is attached

to the balance by means of two ball bearings located near the
Magnus flexures. Model spin is obtained by a two-stage air
turbine which is capable of spinning the model to speeds
well over 500 revolutions per second. The air supply for the
turbine enters through a passageway in the interior of the sting
and exits from the final turbine stage through the base of the
model. A magnetic tachometer, usually located in the forward
portion of the model, provides an analog signal proportional to
the spin rate. There are, of course, the usual provisions for
strain gage signal outlets.

The experimental procedure which is used here is as follows:
The model is mounted on the balance in the test section of the
wind tunnel. After flow is established, the model and support
are rotated to a predetermined angle of attack. Air is then
admitted into the air motor which spins the model to an upper
speed limit of about 500 revolutions per second. The air supply
is then terminated allowing the model spin to decay due to
bearing friction and aerodynamic roll damping. The analog
signals from the strain gages and the magnetic tachometer are
sampled at about 80 times per second as the model undergoes
spin decay. A discussion on how these sampled signals are used
will be deferred until the next section.

Since the Magnus effect on a body without fins is essentially
a viscous phenomenon (see ref. (1)), it is important to be
able to make data comparisons at comparable Reynolds numbers
under the conditions of the test and under conditions of anticipated
projectile operation. Figure 9 is a plot of the Reynolds number
per foot, as a function of Mach number, for the Naval Ordnance
Laboratory's Supersonic Tunnel No. 1. This graph follows from
equation B-3 of reference (2) where the Reynolds number per
foot, $R_{e/\ell}$, is expressed as a function of Mach number and of

the pressure, temperature and viscosity. For reference, this
equation is

$$\frac{R_e}{\ell} = \frac{P_o M}{\mu_o} \sqrt{\frac{\gamma}{(\gamma-1)C_v T_o}} \left(\frac{T_o}{T}\right)^{\frac{\gamma-2}{\gamma-1}} \frac{\frac{T}{T_o} + \frac{198.6}{T_o}}{1 + \frac{198.6}{T_o}} , \quad (1)$$

where μ_o, P_o, M, C_v, T_o and γ are the viscosity at total

conditions, total pressure, Mach number, specific heat at constant
volume, total temperature and the ratio of the specific heats.

Also contained in figure 9 is the equivalent density altitude for the test section conditions. The equivalent density altitude assumes an isothermal atmosphere which for a diatomic gas may be expressed as,

$$h = \frac{5(C_p-C_v)T_O}{2} \ln \left(1 + \frac{M^2}{5} \right) \quad , \tag{2}$$

where the total temperature, T_O, is nominally assumed to be 535 degrees Rankine for the Naval Ordnance Laboratory's Supersonic Tunnel No. 1.

DATA REDUCTION

The Magnus force, $\vec{F_y}$, will be defined as a force dependent

on body spin rate and acting normal to the plane established by the spin vector, $\vec{p}$, and the velocity vector $\vec{V}$. Mathematically this force and its corresponding moment M_z, can be expressed as,

$$\vec{F_y} = K(\vec{p} \times \vec{V}) \tag{3}$$

and

$$\vec{M_z} = K \{\vec{r} \times (\vec{p} \times \vec{V})\} \tag{4}$$

where K is a scalar that is constant for a given set of flow conditions and $\vec{r}$ is the vector from the center of gravity to the Magnus center of pressure. A pictorial representation of equations (3) and (4) is given in figure 1.

All forces and moments used in this definition and measurement are referred to an aeroballistic axis system. This system is a modified body axis system which shares all body motion except spin. As indicated in figure 1, the x axis is forward along the axis of symmetry; the y axis is to the right when the projectile is viewed in the positive x direction; and, the z axis completes a right hand orthogonal triad. The origin of this axis system is at the body's center of gravity. Unit vectors along the x, y and z axes are {i, j, k} Wind tunnel constraints are such that the x-z plane is vertical and contains the flow velocity vector. The spin rate, $\vec{p}$, and the body's velocity vector, $\vec{V}$, may be written as

$$\vec{p} = p\vec{i} \tag{5a}$$

and

$$\vec{V} = V \cos\alpha\vec{i} + V \sin\alpha\vec{k}. \tag{5b}$$

After inserting equations (5) into equations (3) and (4), the Magnus force and moment may be written as

$$\vec{F}_y = -K(pV\sin\alpha)\vec{j} \tag{6}$$

and

$$\vec{M}_z = -K(prV\sin\alpha)\vec{k} . \tag{7}$$

Equation (6) demonstrates that the Magnus force, F_y, is an odd function of the angle of attack and spin rate which generally acts along the negative y axis. Equation (7) points out that the Magnus moment is an odd function of the center of pressure location, spin rate and angle of attack. Equation (7) also states that for a Magnus force acting ahead of the center of gravity (and for positive spin rate) the Magnus moment is negative; i.e., the moment tends to move the missile nose to the left (as viewed from the rear).

The Magnus force and Magnus moment coefficients are defined as

$$\frac{F_y}{QS} = C_y \tag{8a}$$

and

$$\frac{M_z}{QSd} = C_n \tag{8b}$$

Similar relationships can be written for the normal force and pitching moment coefficients as

$$\frac{-F_z}{QS} = C_N \tag{9a}$$

and

$$\frac{M_y}{QSd} = C_m . \tag{9b}$$

7

The coefficients in equations (8) and (9) depend upon the pressure distribution about the body. This pressure distribution, in turn, depends upon the compressibility, unsteadiness and viscosity of the flow. To consider simulation of these effects in a wind tunnel, it is necessary to present coefficients as functions of the appropriate similarity parameters.

Since the free-stream velocity of the medium is in the vicinity of the speed of sound propagation, it is necessary to regard the flow as compressible. Simulation of compressibility effects is assured by testing at the same Mach number. Also, as the Magnus effect on a body without fins originates in the boundary layer, it is necessary to test at the same Reynolds number to simulate viscous effects. Finally, since each surface element on a steadily spinning body at an angle of attack experiences a cyclically changing flow field, it is necessary to test so that there is a parameter which describes the flow unsteadiness. In Magnus tests this flow unsteadiness parameter is designated as the reduced frequency, p. Testing two geometrically similar bodies at identical reduced frequencies assures matching the flow angularity and its rate of change at similarly located body elements. Thus, it is a basic assumption of Magnus testing that the pressure distribution is identical for geometrically similar bodies tested at the same angle of attack for flow conditions in which the Mach number, Reynolds number and reduced frequency are also identical.

Acceptance of the above assumptions is equivalent to saying that the Magnus force and moment coefficients are functions of Mach number, M, Reynolds number, R_e, reduced frequency, $\tilde{p}$, and angle of attack, α. Thus, the Magnus force and moment coefficients may be written as

$$C_y = C_y (M, R_e, \tilde{p}, \alpha) \tag{10a}$$

and

$$C_n = C_n (M, R_e, \tilde{p}, \alpha) \tag{10b}$$

While the above functional relationships might be acceptable, it is not obvious how to describe these functions analytically. In order to accomplish this the experimental technique must be recalled. In making Magnus measurements all variables are held constant (i.e., Mach number, Reynolds number and angle of attack) while loads are measured for a steadily decreasing spin rate. This suggests rewriting equation (10a) as a Taylor series expansion in reduced frequency, $\tilde{p}$ as,

8

$$C_y \ (M, \ R_e, \ \alpha, \ \tilde{p}) = \frac{\partial C_y}{\partial \tilde{p}} \ \tilde{p} + \frac{1}{2!} \ \frac{\partial^2 C_y}{\partial \ \tilde{p}^2} \ \tilde{p}^2 + \frac{1}{3!} \ \frac{\partial^3 C_y}{\partial \ \tilde{p}^3} \ \tilde{p}^3 + \ldots + \frac{1}{n!} \frac{\partial^n C_y}{\partial \ \tilde{p}^n} \ \tilde{p}^n \ . \ (11$$

It should be evident that the term, $C_y \ (M, \ R_e, \ \alpha, \ o)$ is zero since the Magnus effect vanishes for zero spin rate on spin stabilized bodies. In equation (11) the derivatives are functions of the Mach number, M, Reynolds number, R_e, and the angle of attack, α. These derivatives are, of course, evaluated at $\tilde{p}$ equal to zero.

It will be shown subsequently that the Magnus force and moment coefficients are linear with the reduced frequency. In this case equation (11) takes on the simpler form,

$$C_y = C_y \ (M, \ R_e, \ \alpha, \ \tilde{p}) = \frac{\partial C_y}{\partial \ \tilde{p}} \ \tilde{p} \equiv C_{y_p} \ \tilde{p} \tag{12a}$$

with the corresponding expression for the moment being,

$$C_n = C_n \ (M, \ R_e, \ \alpha, \ \tilde{p}) = \frac{\partial C_n}{\partial \ p} \ \tilde{p} \equiv C_{n_p} \ \tilde{p} \tag{12b}$$

It is the purpose of the data reduction, then, to obtain the derivatives C_{y_p} and C_{n_p} as direct functions of the angle of attack and as indirect functions of Mach number. Assuming for the moment that the above linearization is justified, it is of interest to see what the data reduction procedure is.

In figure 10 the model is indicated to be in the wind tunnel subject to preset flow conditions. The analog signals from the strain gages and the magnetic tachometer are sampled approximately 80 times per second. These samples are converted into digital form and recorded on magnetic tape. This magnetic tape, together with the balance static calibration, is processed through a digital computer program so as to obtain the Magnus force and Magnus moment coefficients as discrete functions of the reduced frequency, $\tilde{p}$. These two coefficients and the reduced frequency are recorded on a plot tape. The plot tape, in conjunction with an automatic plotter, provides a graphical presentation of these coefficients versus the reduced frequency. In the case of bodies without fins these data show sufficient linearity to justify the fitting of a straight line through the data points by the method of a least squares fit. The slope of this straight line then becomes the Magnus force and Magnus moment derivatives, C_{y_p} and C_{n_p}. Since these Magnus derivatives are obtained at fixed values of Mach number, Reynolds number and

9

angle of attack, any change in one of these variables results
in different values for these derivatives. In Supersonic
Tunnel No. 1, Reynolds number could not be independently
varied; thus, the Magnus derivatives are presented only as
functions of angle of attack and Mach number.

RESULTS

In the preceding section it was mentioned that the data
reduction was based upon an assumption of linearity between the
Magnus force and moment and the reduced frequency. While it is
not necessary to present graphs of the Magnus coefficients,
C_y and C_n, versus the reduced frequency, one such plot will be

presented to support the linear assumption.

Figure 11 is a plot of the Magnus moment coefficient, C_n,
versus the reduced frequency, p. It can be seen from this
figure that the Magnus moment may be adequately represented as
a linear function of the reduced frequency.

Figures 12 through 20 present the Magnus force and moment
derivatives, C_{y_p} and C_{n_p} respectively, as functions of angle of

attack for the 7-, 8-, 9- and 10-caliber slender bodies. It will
be noted in these figures that the Magnus force and moment
coefficients are quite nonlinear with angle of attack. There
is also the expected trend of a decrease in the Magnus force
and moment characteristics with Mach number.

Figure 21 is a presentation of the Magnus moment derivative
versus angle of attack measured at a Mach number of 2.0 for the
four slender bodies. This figure clearly indicates the effect
of body length on the Magnus moment derivative. It is interesting
to note the effect of body length on the center of pressure location.
Using figures 12 through 20, the Magnus center of pressure at a
Mach number of 2.0, and at an angle of attack of 12 degrees, is
5.2-calibers aft of the nose on the 7-caliber body. For the
8-, 9- and 10-caliber bodies it is at 6.1-, 6.5- and 7.5-calibers,
respectively. Incidentally, the moment reference center for
all moment measurements is the body vertex.

Figures 22 through 27 present the static aerodynamic force
and moment characteristics for the four slender bodies. All static
measurements were found to vary about 5 percent or less over
the entire range of reduced frequencies tested. All measurements
presented in figures 22 through 27 were made for a nominal reduced
spin rate of 0.060.

REFERENCES

(1) Martin, John C., "On Magnus Effects Caused by the Boundary Layer Displacement Thickness on Bodies of Revolution at Small Angles of Attack," Journal of the Aeronautical Sciences, June 1957.

(2) Ames Research Staff, "Equations, Tables and Charts for Compressible Flow," NACA Report 1135, 1953.

BLANK PAGE
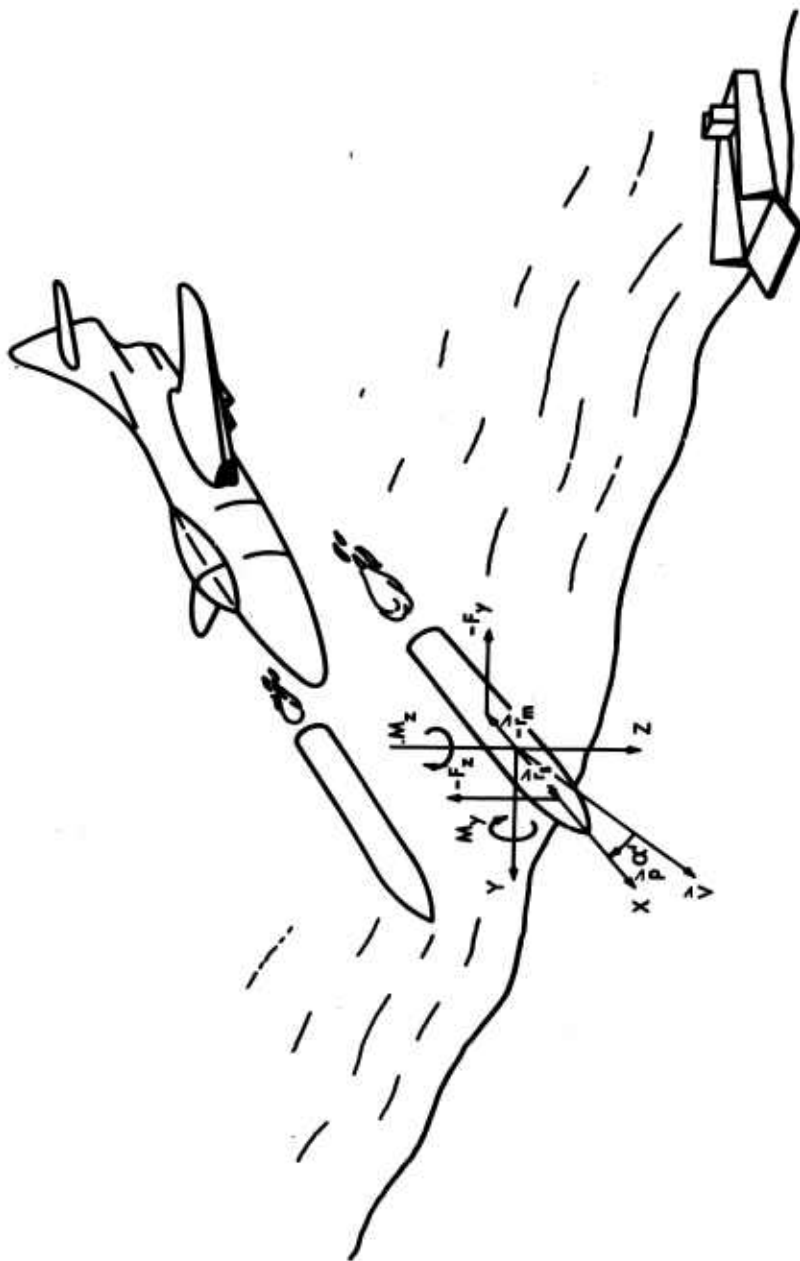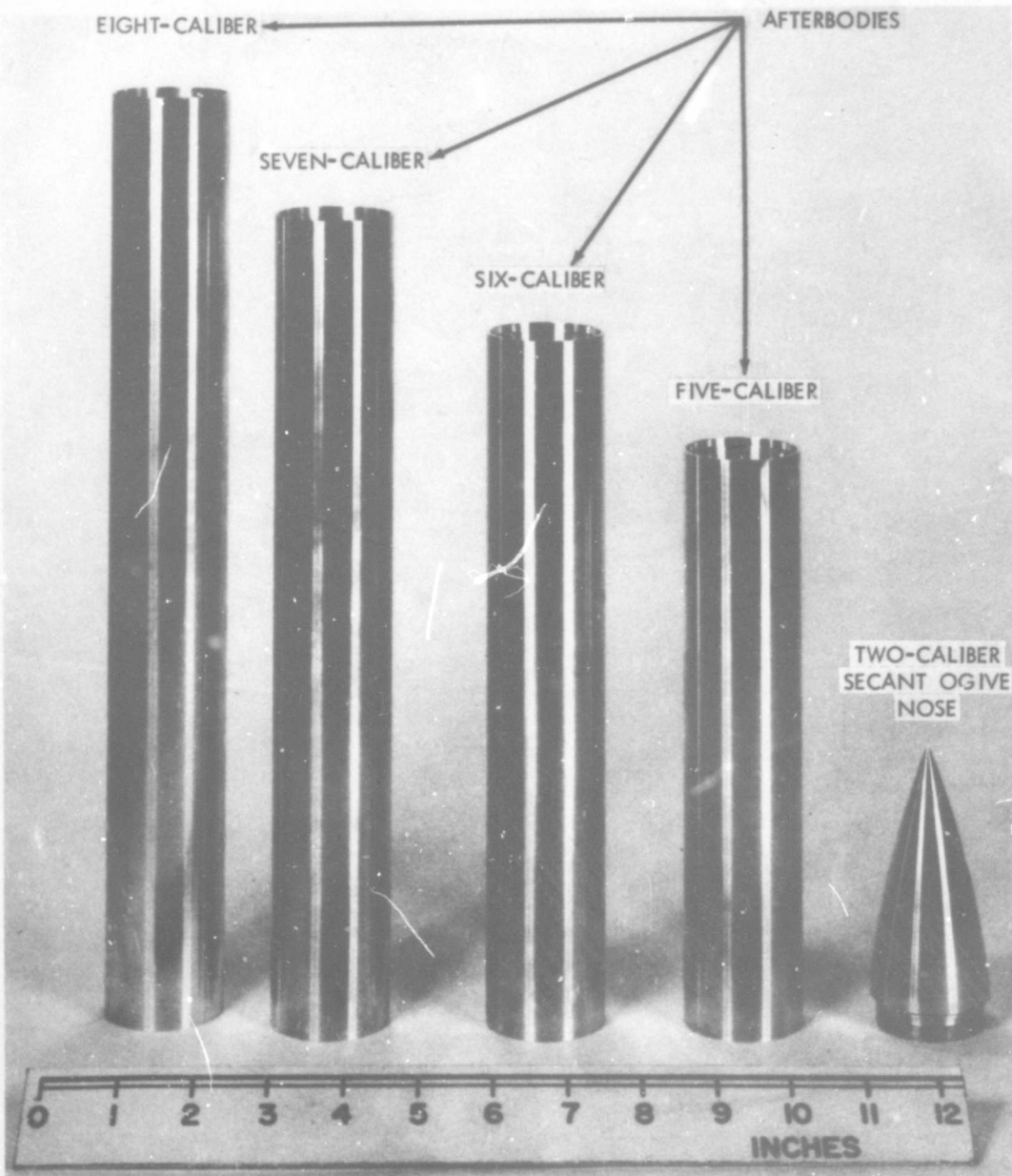
FIG. 1 SLENDER BODY USED AS A ROCKET ASSISTED PROJECTILE

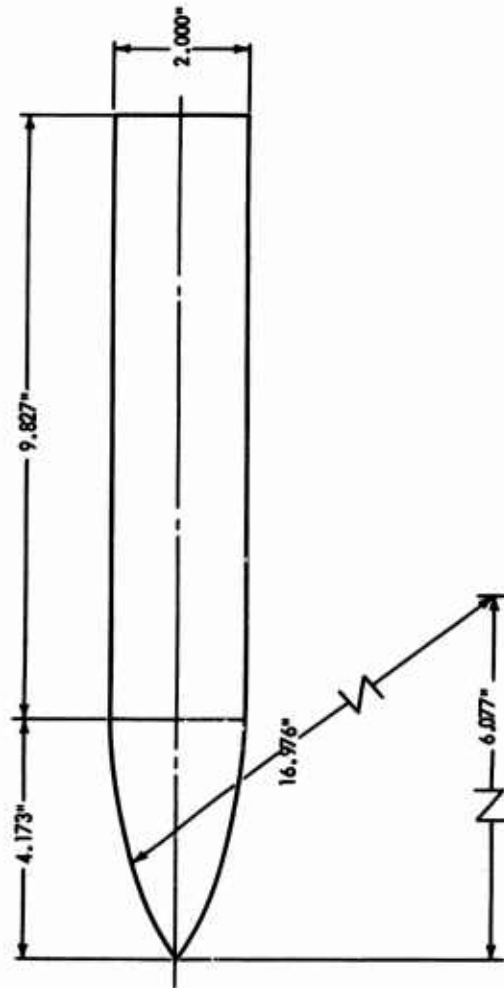FIG. 2 WIND TUNNEL MODELS USED IN SLENDER BODY MAGNUS STUDY

FIG. 3 EXTERNAL DIMENSIONS OF THE SEVEN-CALIBER
WIND TUNNEL MODEL

TACH AND GAGE READOUT
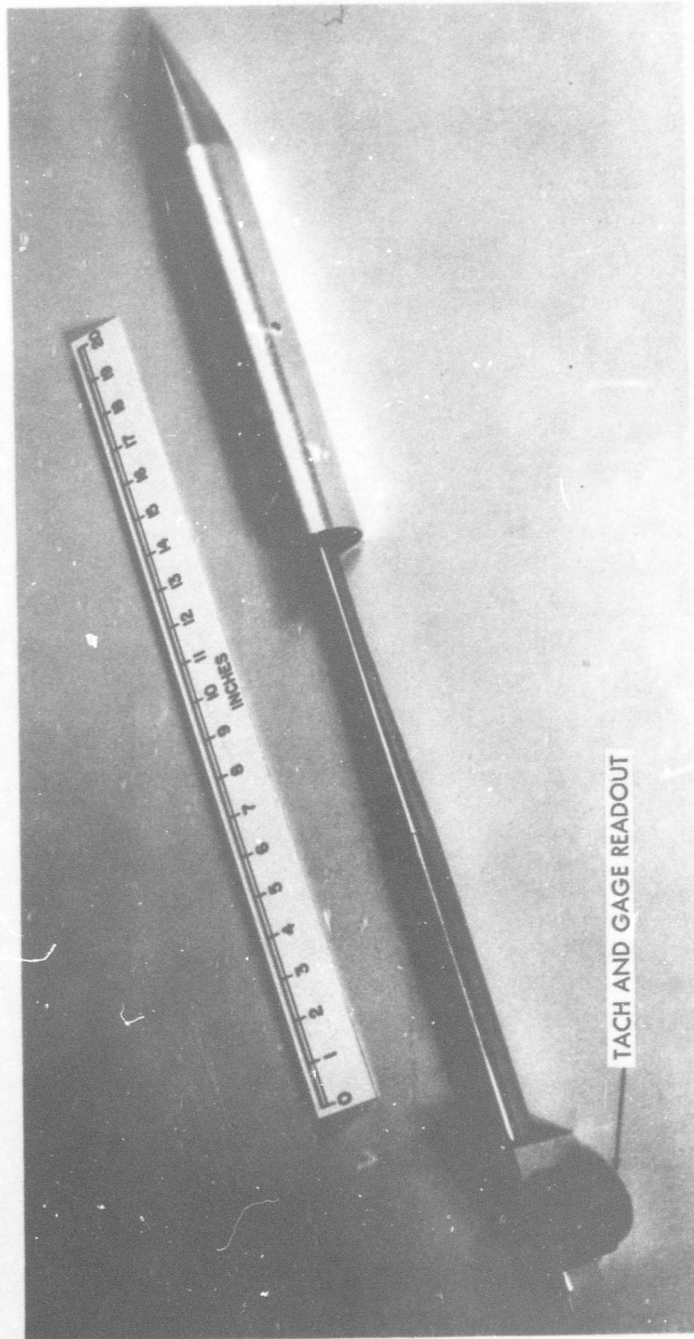
FIG. 4 SEVEN-CALIBER SLENDER BODY MODEL ON MAGNUS BALANCE
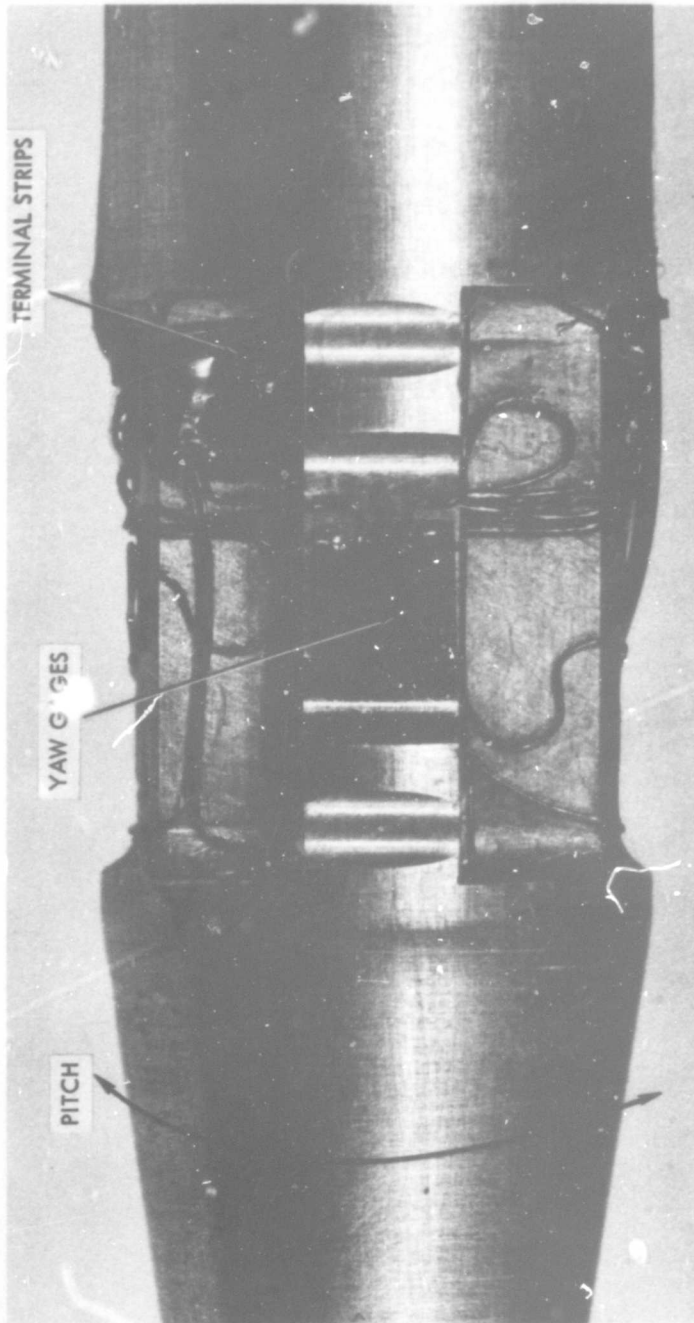
FIG. 5 PITCH PLANE VIEW OF FORWARD GAGE SECTION OF MAGNUS BALANCE
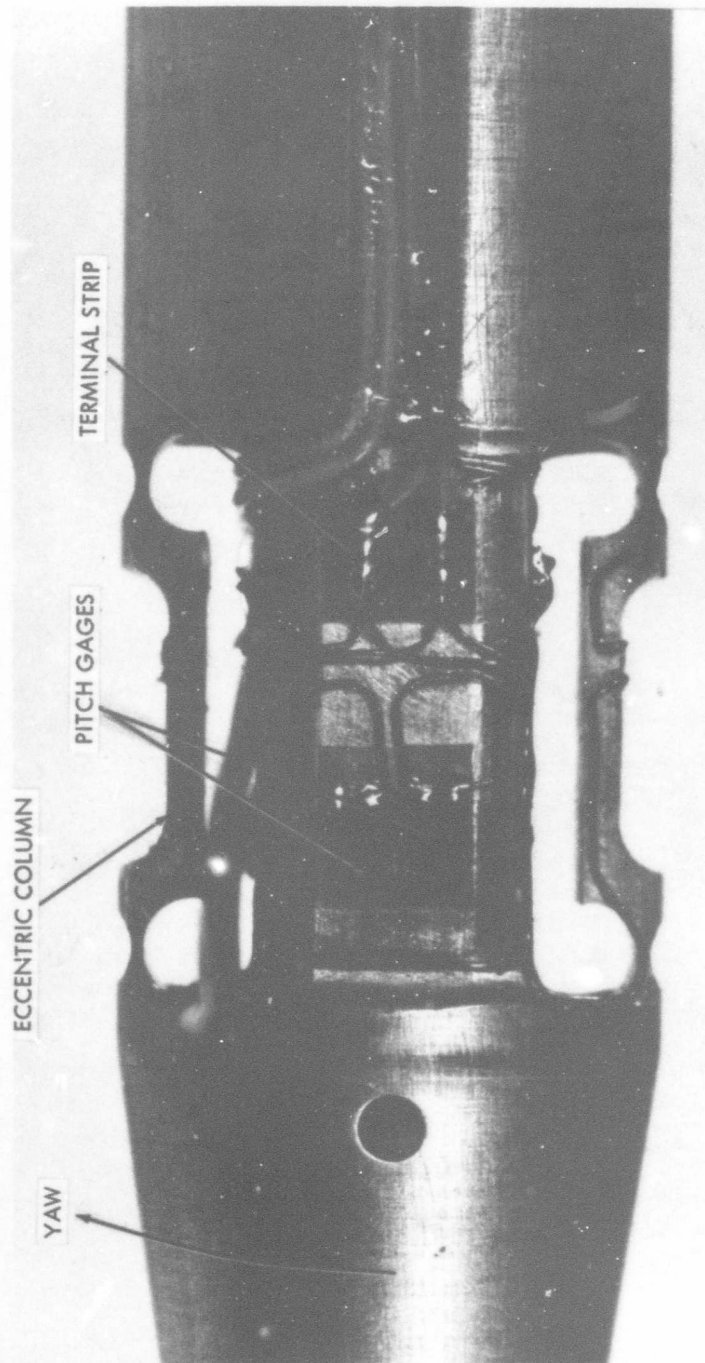
FIG. 6 YAW PLANE VIEW OF FORWARD GAGE SECTION OF MAGNUS BALANCE
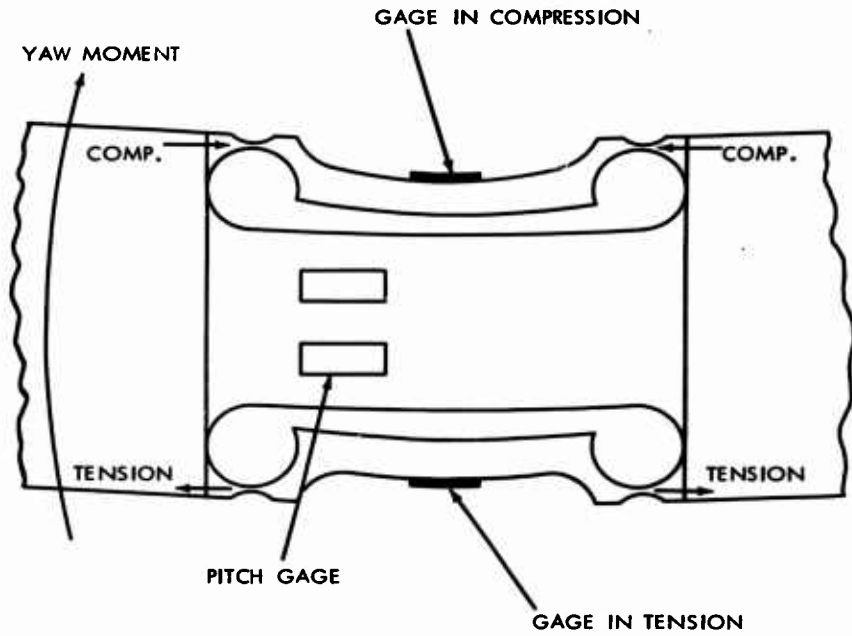
FIG. 7 MAGNUS BRIDGE UNDER YAW MOMENT
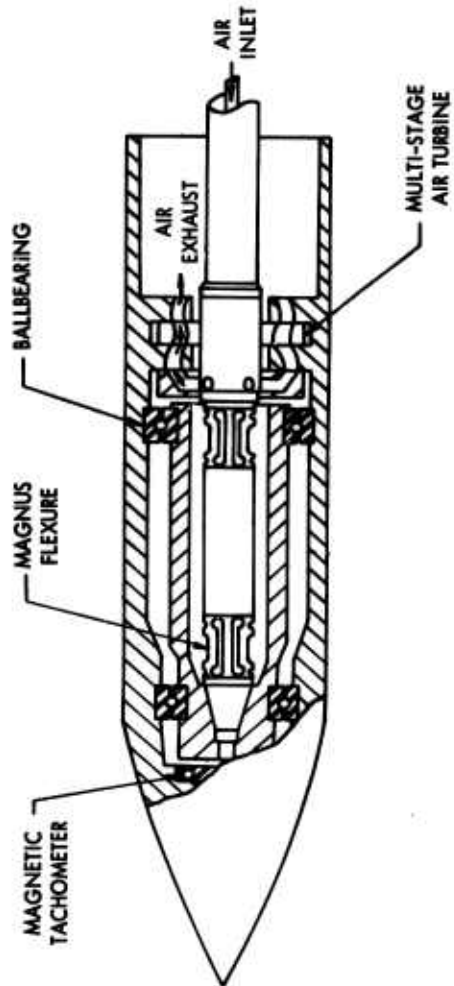
FIG. 8 MAGNUS BALANCE DETAILS
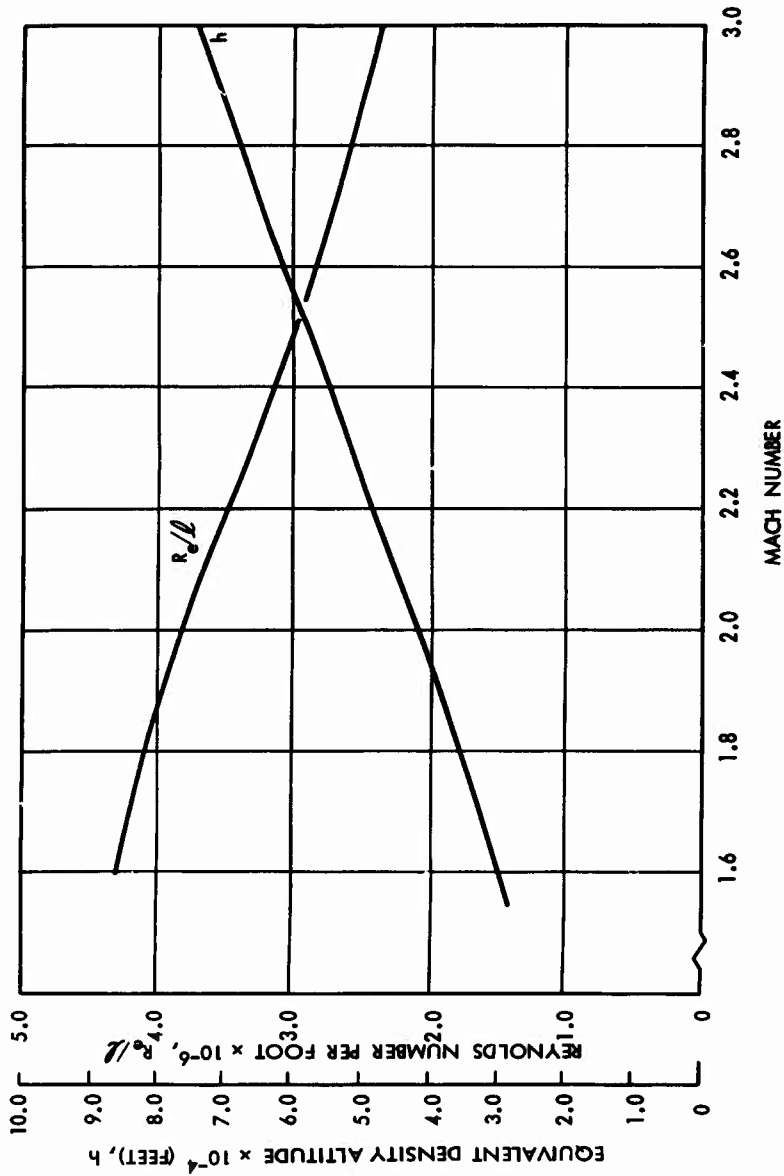
FIG. 9 REYNOLDS NUMBER PER FOOT AND EQUIVALENT DENSITY ALTITUDE VERSUS MACH NUMBER FOR U.S. NAVAL ORDNANCE LABORATORY SUPERSONIC TUNNEL NO. 1
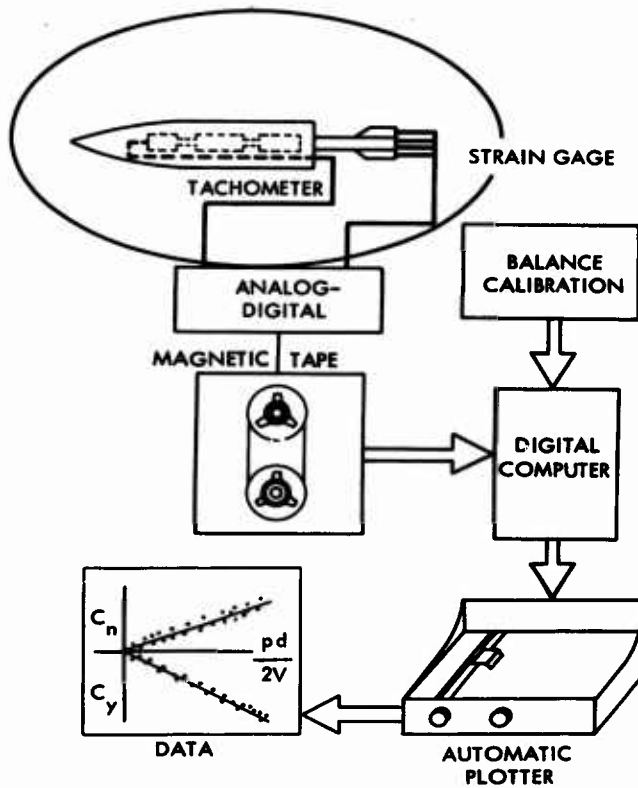
FIG.10 DATA ACQUISITION AND REDUCTION
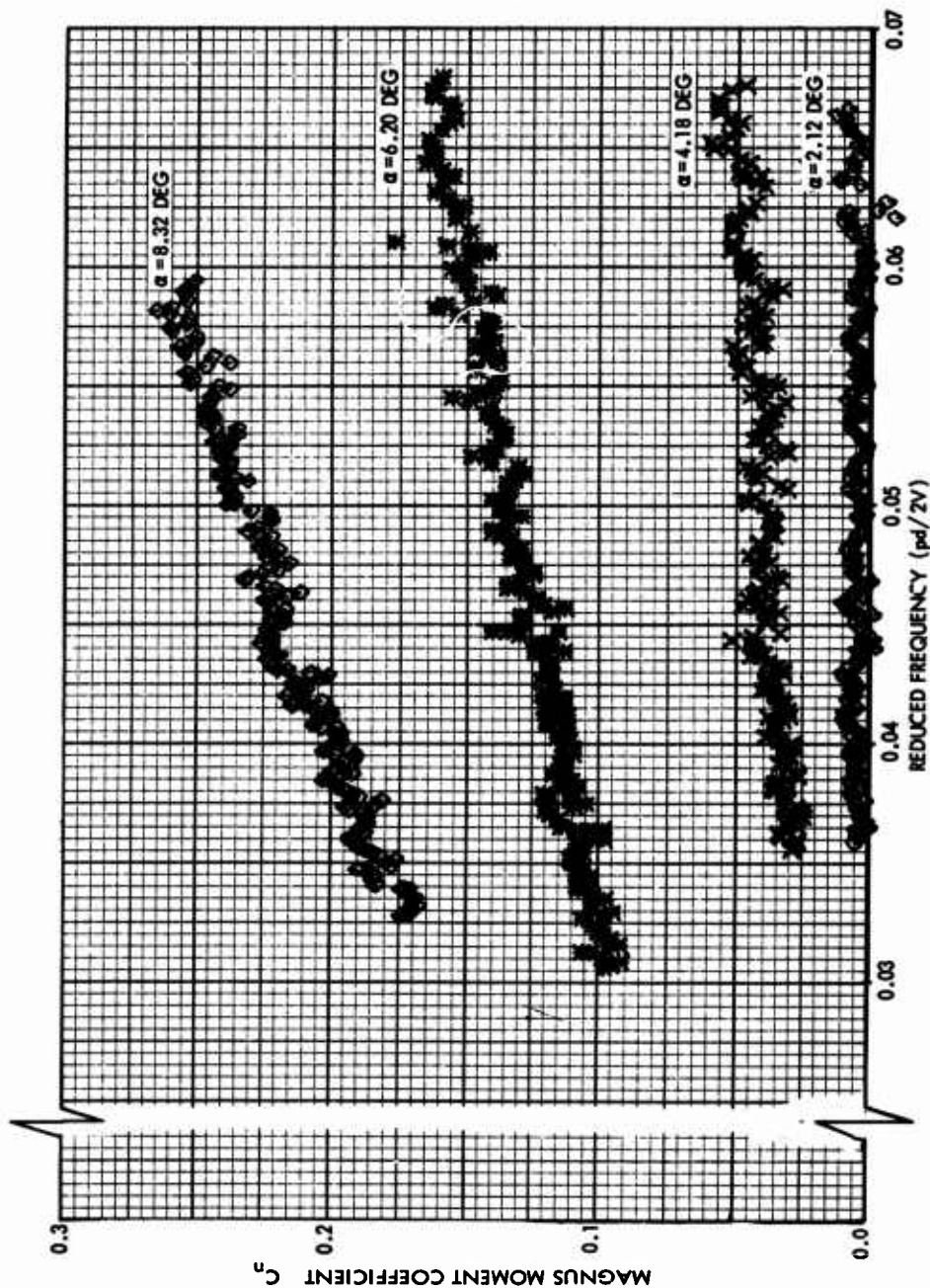
FIG. 11 MAGNUS MOMENT COEFFICIENT VERSUS REDUCED FREQUENCY FOR THE
8-CALIBER SLENDER BODY AT A MACH NUMBER OF 2.0
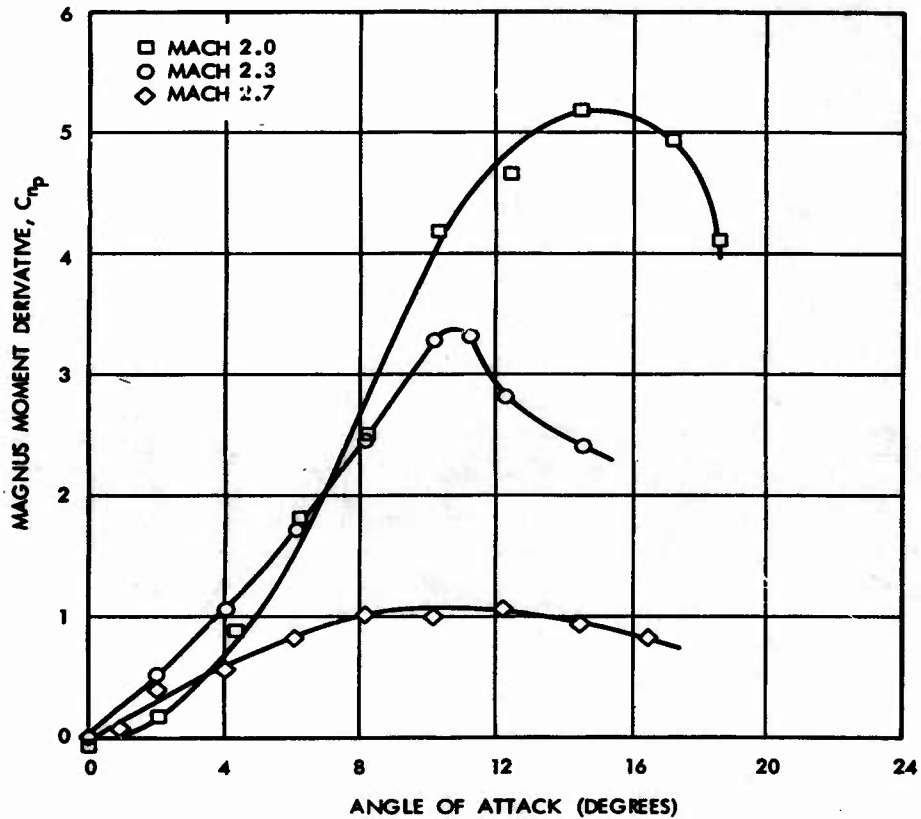
FIG. 12 MAGNUS MOMENT DERIVATIVE VERSUS ANGLE OF
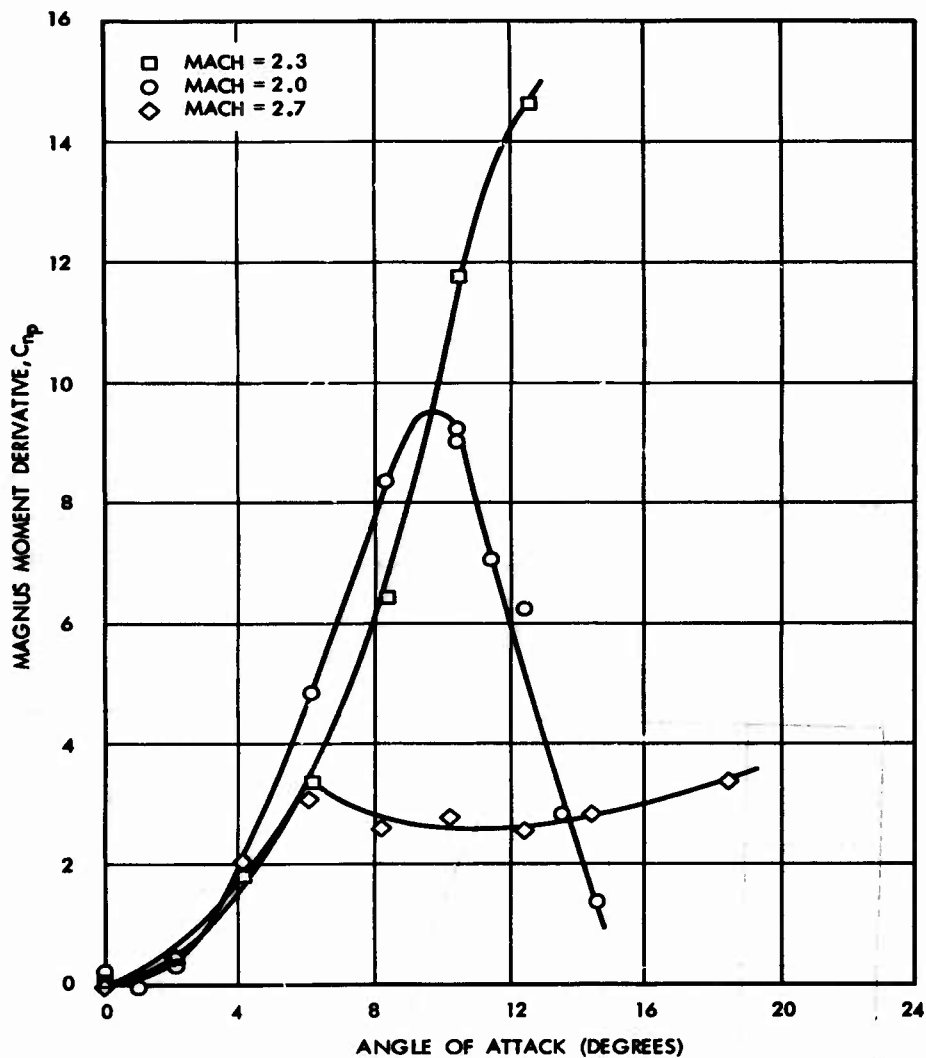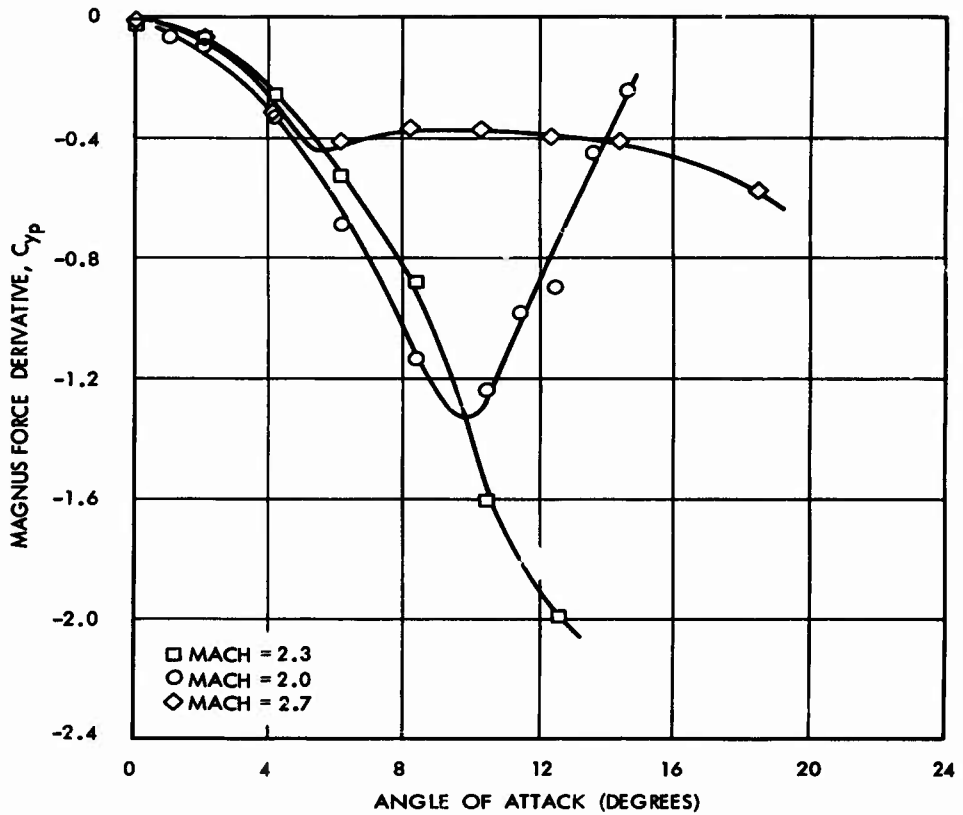ATTACK FOR SEVEN-CALIBER SLENDER BODY
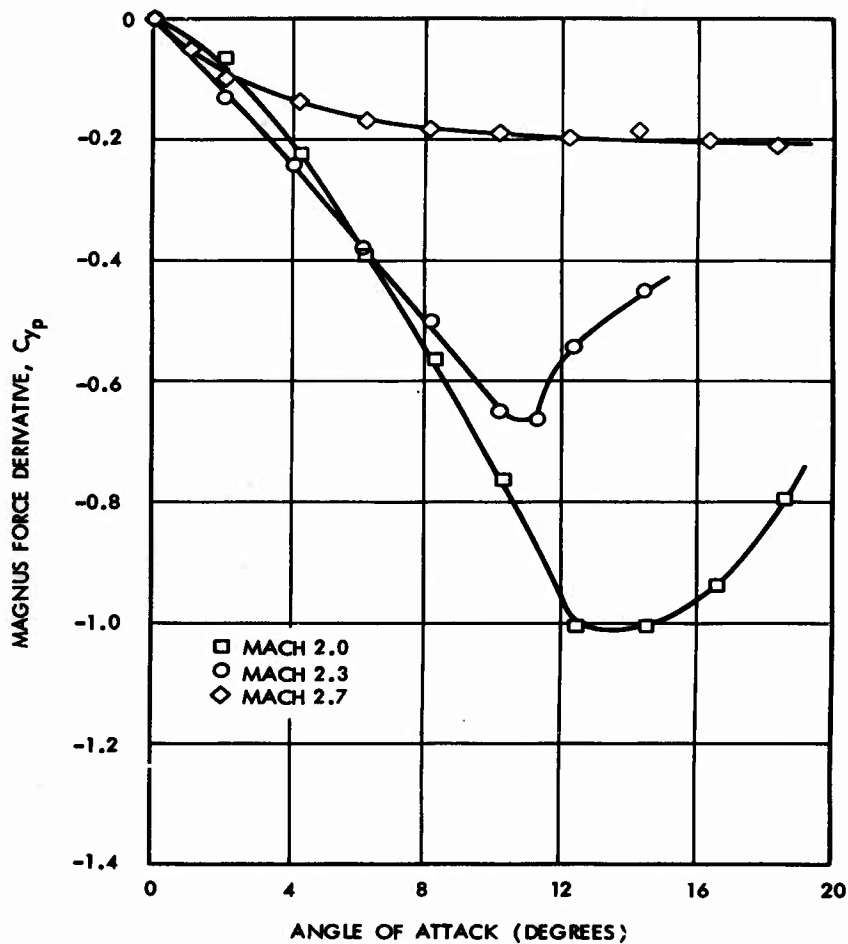
FIG. 13 MAGNUS FORCE DERIVATIVE VERSUS ANGLE
OF ATTACK FOR SEVEN-CALIBER SLENDER BODY
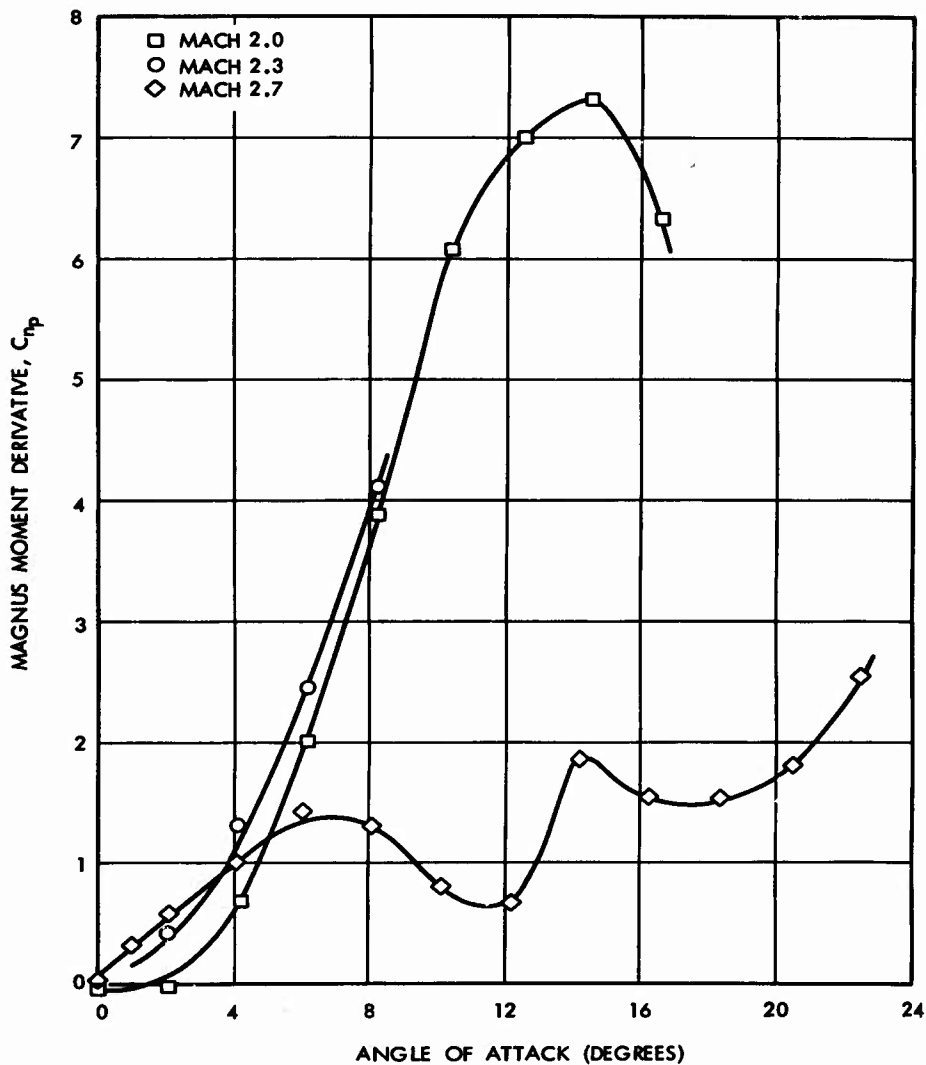
FIG. 14 MAGNUS MOMENT DERIVATIVE VERSUS ANGLE OF
ATTACK FOR EIGHT-CALIBER SLENDER BODY
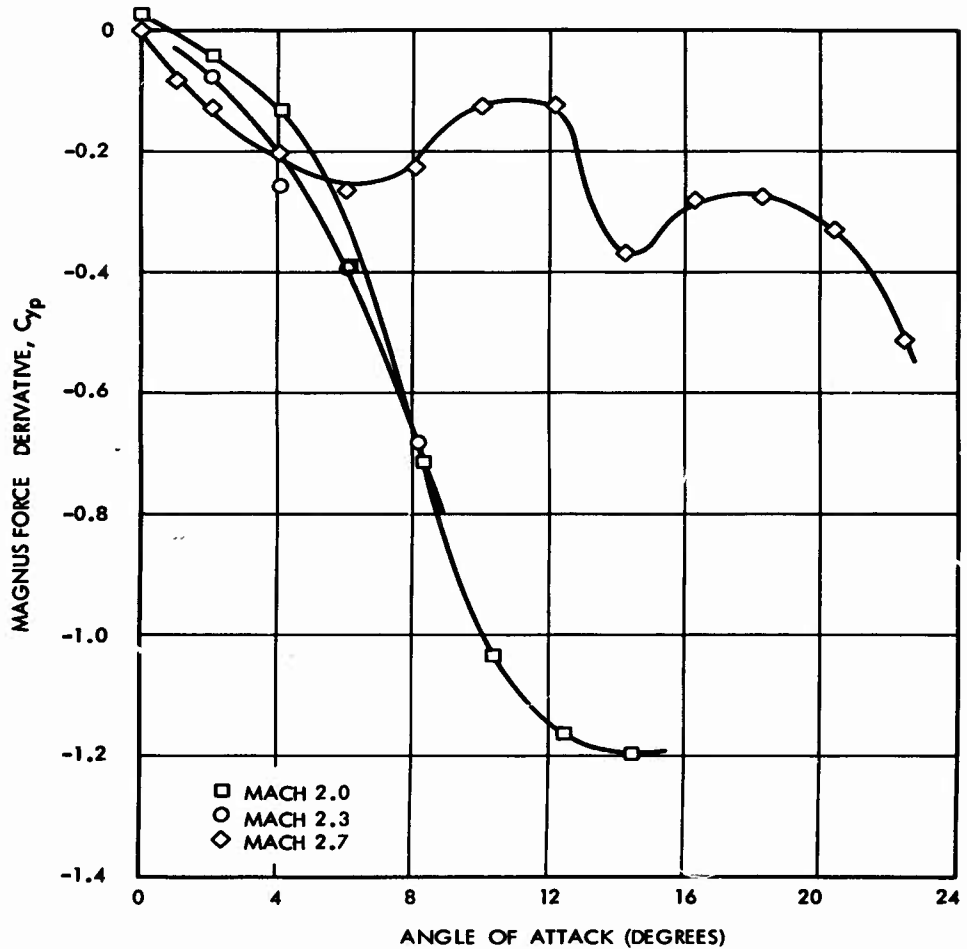
FIG. 15   MAGNUS FORCE DERIVATIVE VERSUS ANGLE OF
ATTACK FOR EIGHT-CALIBER SLENDER BODY
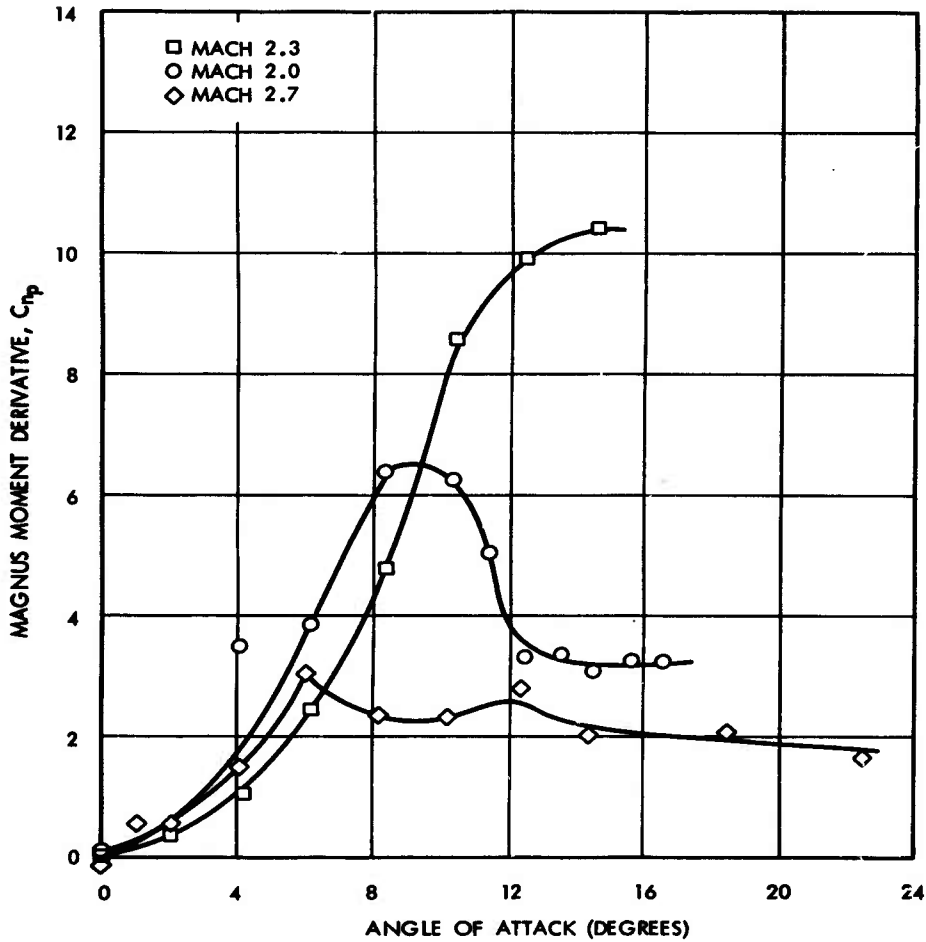
FIG. 16 MAGNUS MOMENT DERIVATIVE VERSUS ANGLE OF
ATTACK FOR NINE-CALIBER SLENDER BODY
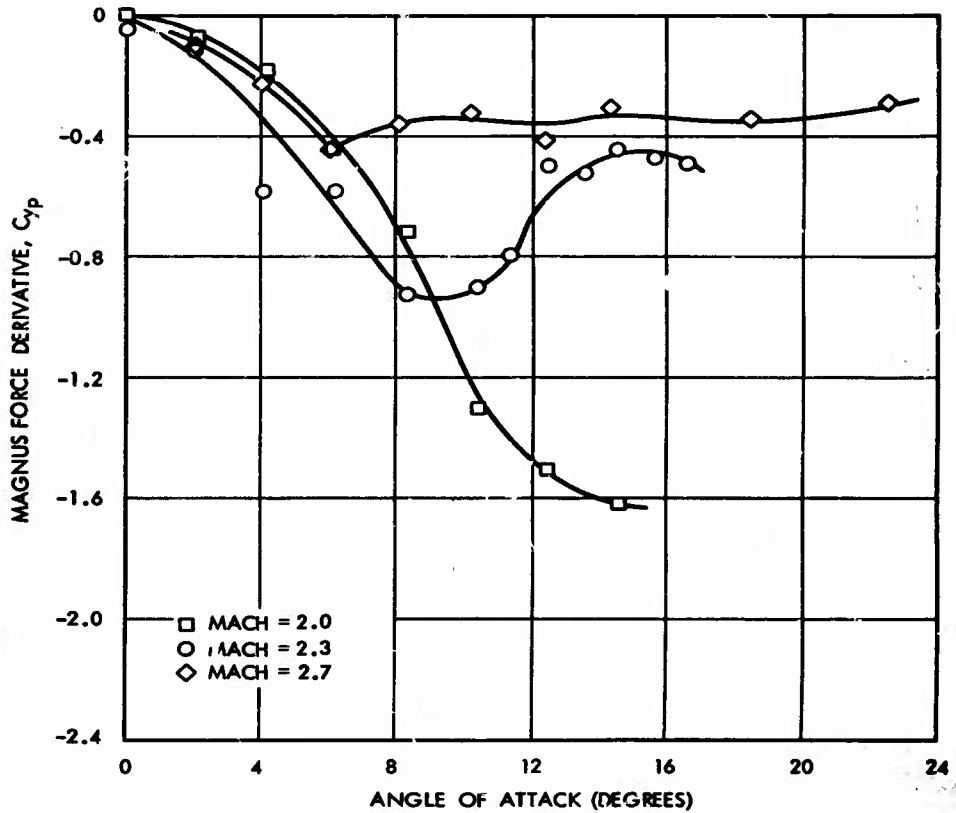
FIG. 17 MAGNUS FORCE DERIVATIVE VERSUS ANGLE OF
ATTACK FOR NINE-CALIBER SLENDER BODY

FIG. 18 MAGNUS MOMENT DERIVATIVE VERSUS ANGLE OF
ATTACK FOR TEN-CALIBER SLENDER BODY.

FIG. 19 MAGNUS FORCE DERIVATIVE VERSUS ANGLE OF
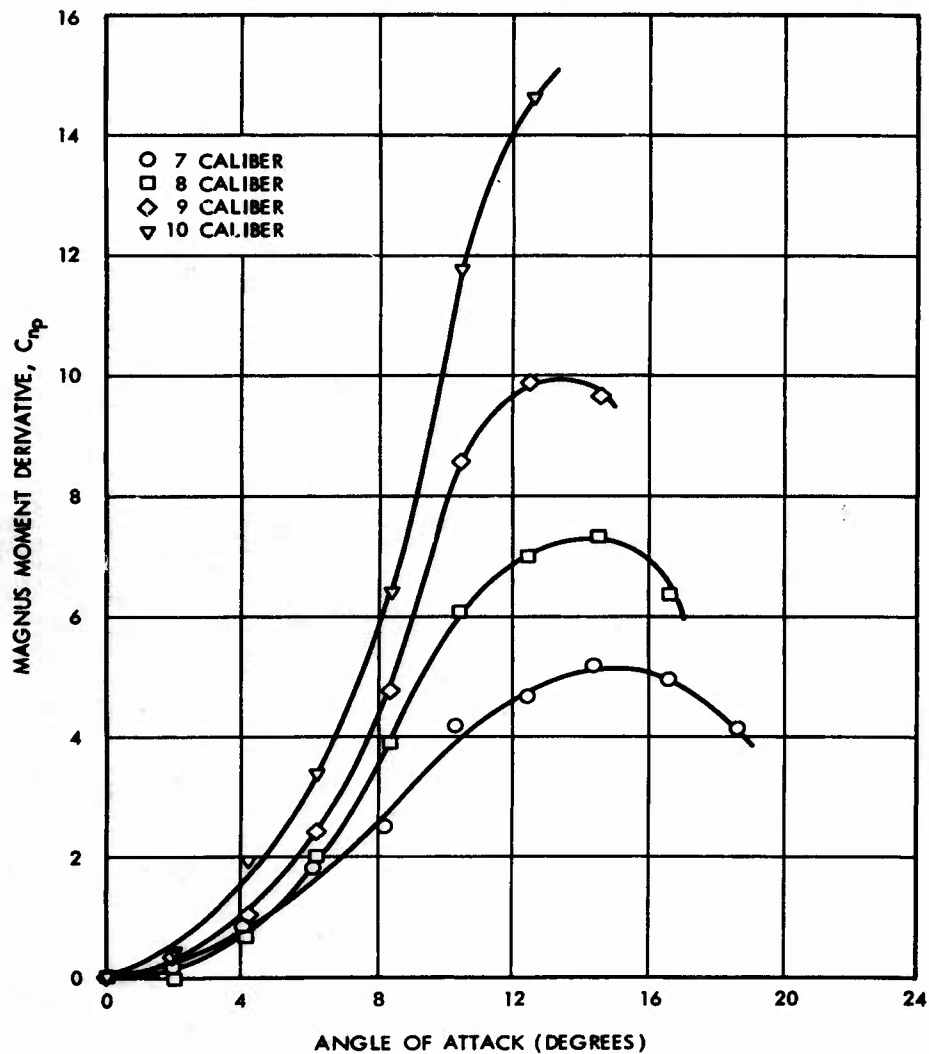ATTACK FOR TEN-CALIBER SLENDER BODY

FIG. 20 MAGNUS MOMENT DERIVATIVE VERSUS ANGLE OF ATTACK
FOR THE SEVEN-, EIGHT, NINE-AND TEN-CALIBER SLENDER
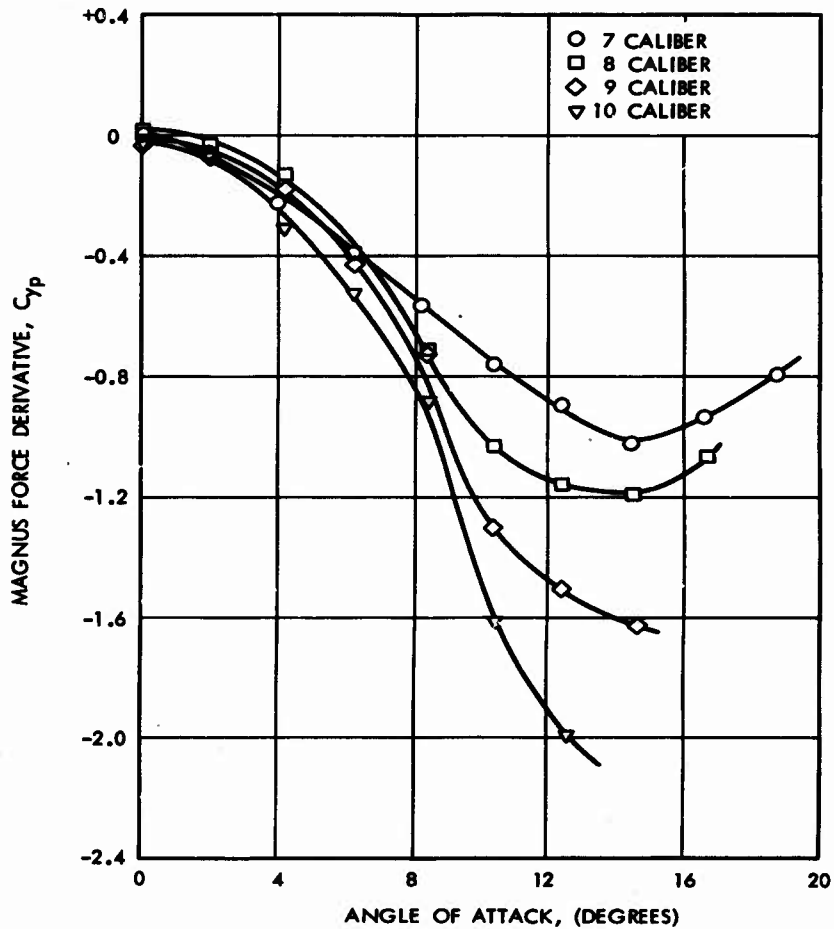BODIES AT MACH 2.0

FIG.21 MAGNUS FORCE DERIVATIVE VERSUS ANGLE OF ATTACK
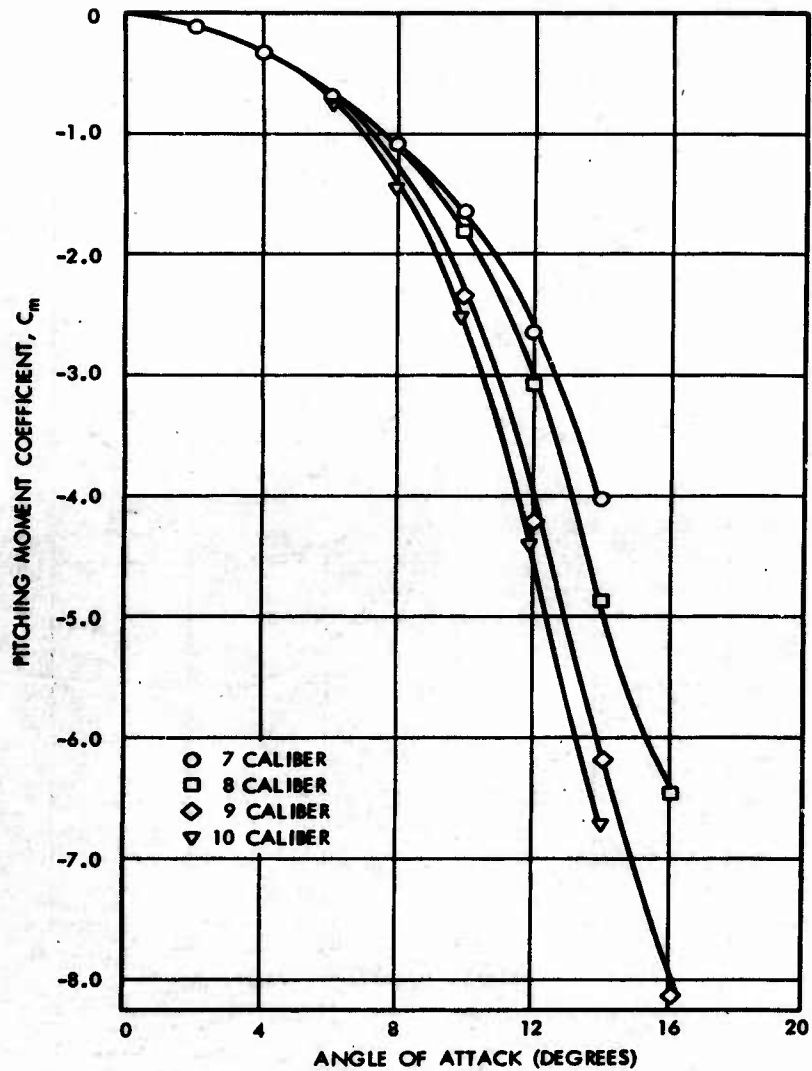FOR THE SEVEN-,EIGHT-,NINE-AND TEN-CALIBER SLENDER
BODIES AT MACH 2.0

FIG. 22 PITCHING MOMENT COEFFICIENT VERSUS ANGLE OF ATTACK FOR
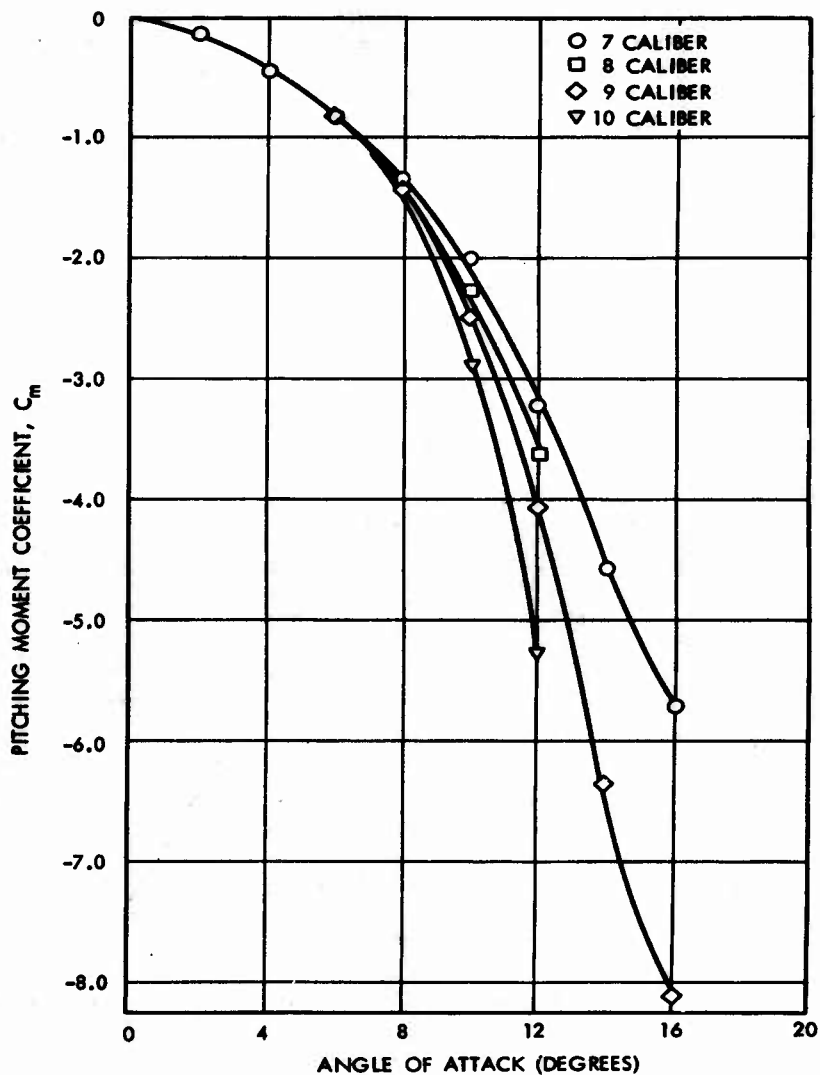THE SEVEN-, EIGHT-, NINE- AND TEN-CALIBER SLENDER
BODIES AT MACH 2.0

FIG. 23 PITCHING MOMENT COEFFICIENT VERSUS ANGLE OF
ATTACK FOR THE SEVEN, EIGHT, NINE- AND TEN-
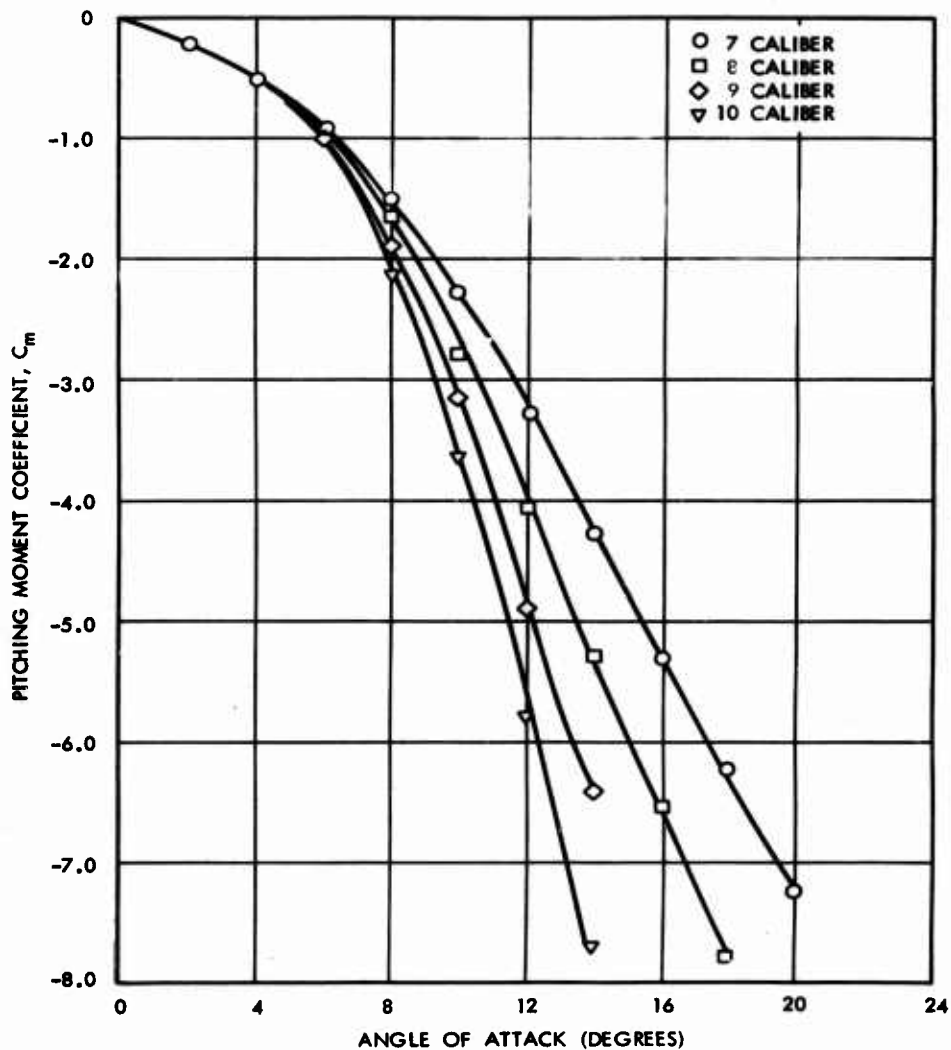CALIBER SLENDER BODIES AT MACH 2.3

FIG.24 PITCHING MOMENT COEFFICIENT VERSUS ANGLE OF ATTACK
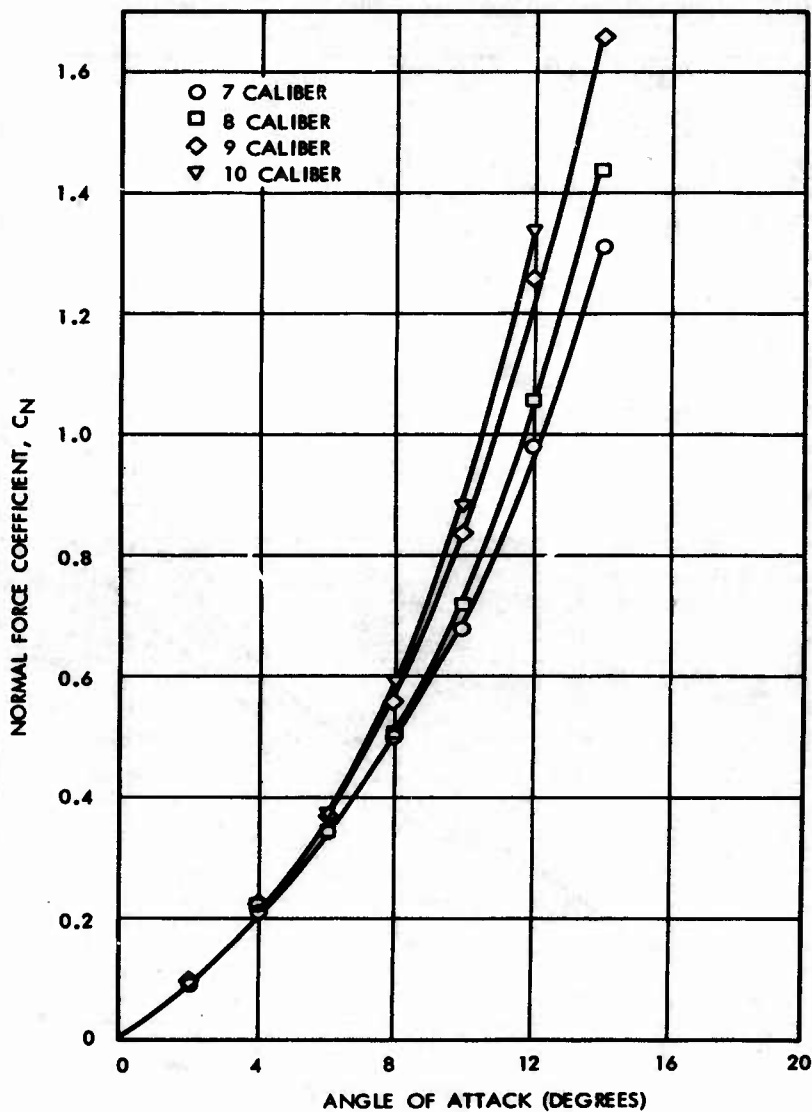FOR THE SEVEN-,EIGHT-, NINE-AND TEN-CALIBER SLENDER
BODIES AT MACH 2.7

FIG. 25 NORMAL FORCE COEFFICIENT VERSUS ANGLE OF ATTACK
FOR THE SEVEN,EIGHT,NINE-AND TEN-CALIBER SLENDER
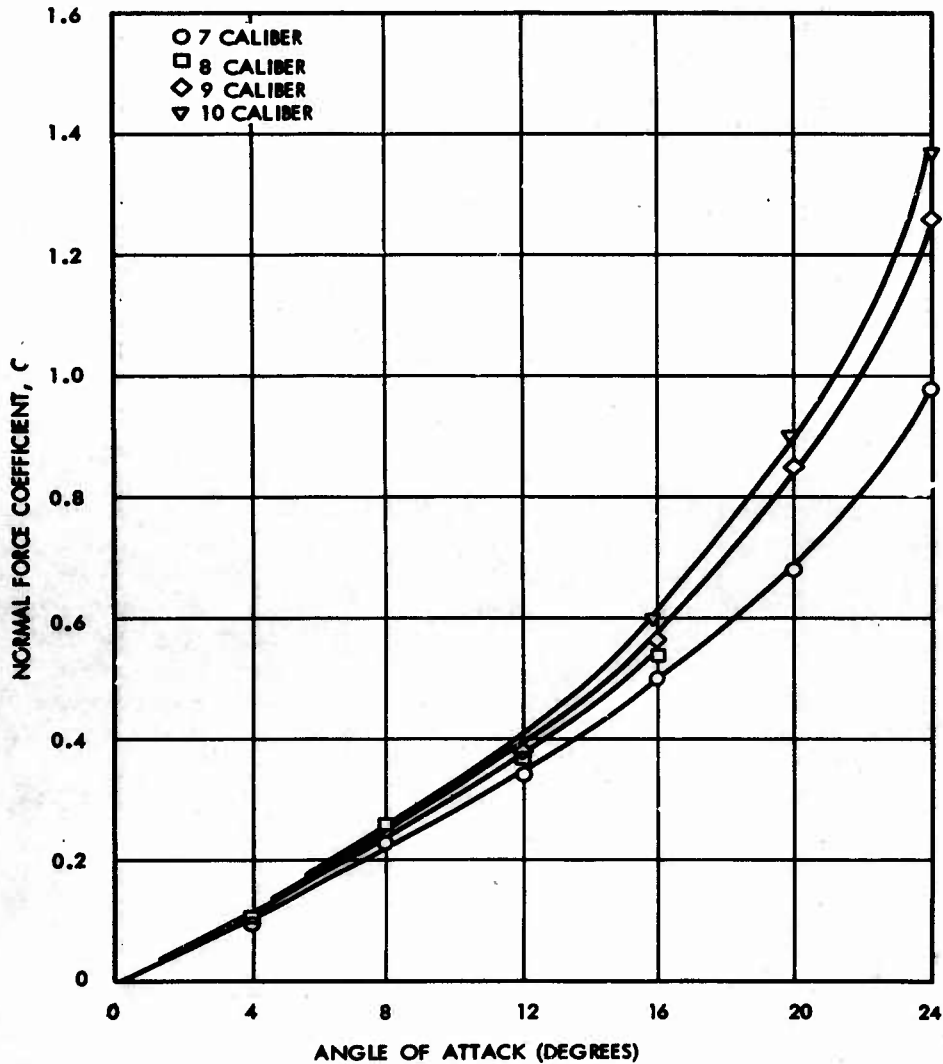BODIES AT MACH 2.0

FIG. 26 NORMAL FORCE COEFFICIENT VERSUS ANGLE OF ATTACK FOR THE SEVEN, EIGHT, NINE- AND TEN-CALIBER SLENDER BODIES AT MACH 2.3
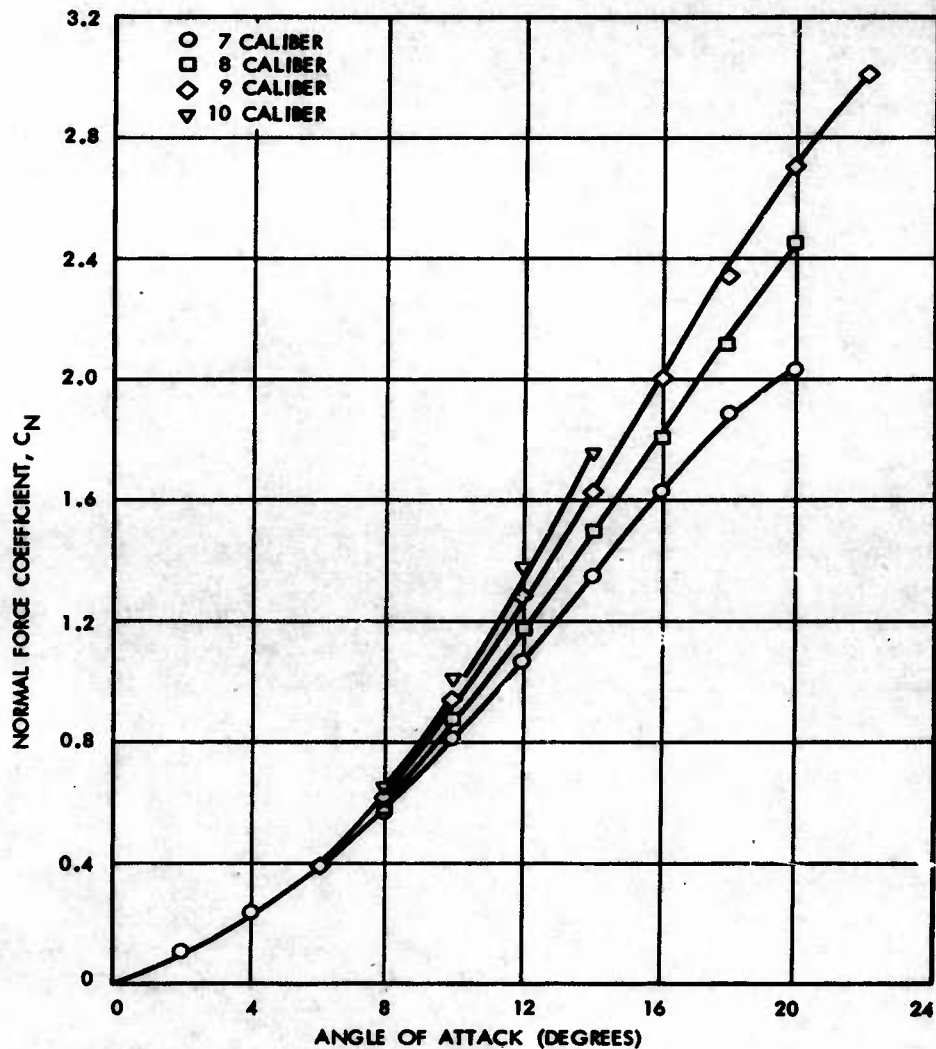
FIG. 27 NORMAL FORCE COEFFICIENT VERSUS ANGLE OF ATTACK
FOR THE SEVEN, EIGHT, NINE-AND TEN-CALIBER SLENDER
BODIES AT MACH 2.7

DOCUMENT CONTROL DATA - R & D

(Security classification of title, body of abstract and indexing annotation must be entered when the overall report is classified)

1. ORIGINATING ACTIVITY *(Corporate author)*	2a. REPORT SECURITY CLASSIFICATION
U. S. Naval Ordnance Laboratory White Oak, Silver Spring, Maryland	UNCLASSIFIED
	2b. GROUP

3. REPORT TITLE

SUPERSONIC WIND TUNNEL MAGNUS MEASUREMENTS OF THE 7-, 8-, 9- AND 10-CALIBER ARMY-NAVY SPINNER PROJECTILE

4. DESCRIPTIVE NOTES *(Type of report and inclusive dates)*

5. AUTHOR(S) *(First name, middle initial, last name)*

John E. Holmes, Frank J. Regan and Mary Ellen Falusi

6. REPORT DATE	7a. TOTAL NO. OF PAGES	7b. NO. OF REFS
10 October 1968	15 plus illust.	2
8a. CONTRACT OR GRANT NO.	9a. ORIGINATOR'S REPORT NUMBER(S)	
b. PROJECT NO.	NOLTR 68-172	
c. Task Number A32 320/292/69F 20311202 WU-3	9b. OTHER REPORT NO(S) *(Any other numbers that may be assigned this report)*	
d.		

10. DISTRIBUTION STATEMENT

This document is subject to special export controls and each transmittal to foreign government or foreign nationals may be made only with prior approval of NOL.

11. SUPPLEMENTARY NOTES	12. SPONSORING MILITARY ACTIVITY
	Naval Air Systems Command Washington, D. C.

13. ABSTRACT

The Army-Navy Spinner Projectile is a research shape that has been used as the foundation of many spin stabilized weapon designs. The purpose of the wind tunnel tests was to make supersonic wind tunnel Magnus measurements on AN Spinner configurations of 7-, 8-, 9- and 10-caliber lengths. Such an experimental study indicates the effect of length on the Magnus force and moment for a basic spin stabilized shape. ( )

14 KEY WORDS	LINK A		LINK B		LINK C	
	ROLE	WT	ROLE	WT	ROLE	WT
Projectile						
Magnus						
Army-Navy Spinner						